APL Materials

Molecular beam epitaxy growth of Al-rich AlGaN nanowires for deep ultraviolet optoelectronics

Cite as: APL Mater. 4, 086115 (2016); https://doi.org/10.1063/1.4961680
Submitted: 12 July 2016 • Accepted: 15 August 2016 • Published Online: 29 August 2016

S. Zhao, S. Y. Woo, S. M. Sadaf, et al.

Molecular beam epitaxy growth of Al-rich AlGaN nanowires for deep ultraviolet optoelectronics

S. Zhao,[1,a] S. Y. Woo,[2] S. M. Sadaf,[1] Y. Wu,[1] A. Pofelski,[2] D. A. Laleyan,[1] R. T. Rashid,[1] Y. Wang,[1] G. A. Botton,[2] and Z. Mi[1,a]
[1]*Department of Electrical and Computer Engineering, McGill University, 3480 University Street, Montreal, Quebec H3A 0E9, Canada*
[2]*Department of Materials Science and Engineering, Canadian Centre for Electron Microscopy, McMaster University, 1280 Main Street West, Hamilton, Ontario L8S 4M1, Canada*

(Received 12 July 2016; accepted 15 August 2016; published online 29 August 2016)

Self-organized AlGaN nanowires by molecular beam epitaxy have attracted significant attention for deep ultraviolet optoelectronics. However, due to the strong compositional modulations under conventional nitrogen rich growth conditions, emission wavelengths less than 250 nm have remained inaccessible. Here we show that Al-rich AlGaN nanowires with much improved compositional uniformity can be achieved in a new growth paradigm, wherein a precise control on the optical bandgap of ternary AlGaN nanowires can be achieved by varying the substrate temperature. AlGaN nanowire LEDs, with emission wavelengths spanning from 236 to 280 nm, are also demonstrated. [http://dx.doi.org/10.1063/1.4961680]

Deep ultraviolet (UV) light sources including light emitting diodes (LEDs) and lasers in the wavelength range of 240 nm are essential for a broad range of applications including surface treatment, biochemical analysis, and medical diagnostics. As of yet, a mature semiconductor technology has been missing for this purpose. AlGaN compound semiconductors, with their wide optical bandgap tunability from 200 to 364 nm, have been intensively investigated for applications in UV LEDs and lasers.[1–13] However, compared to the well-established high performance GaN-based quantum well LEDs and lasers operating in the near-UV, blue, and blue-green spectral ranges, realizing high performance AlGaN quantum well UV LEDs and lasers in the UV-C band (200-280 nm), in particular those emitting below 240 nm, has been extremely challenging.[1–4,13–17] The extraordinary challenges include the presence of large dislocation and defect densities, the extremely inefficient *p*-type conduction due to the large Mg activation energy and doping induced defect donors, and the unique TM light polarization in Al-rich AlGaN.[5–8]

As an alternative path to achieve high efficiency UV LEDs and lasers, AlGaN nanowire structures have drawn considerable attention.[18–30] The promise of AlGaN nanowires stems not only from their low defect densities, but more importantly, their surface enhanced *p*-type dopant (Mg) incorporation. It has been demonstrated, both experimentally and theoretically, that Mg-dopant incorporation is significantly enhanced in AlN, InN, and GaN nanowire structures compared to their bulk counterparts,[26,31–33] thereby promising very efficient *p*-type conduction in wide bandgap Al-rich AlGaN that was not possible previously. However, with the use of conventional chemical vapor deposition processes, Al-rich AlGaN nanowire structures only yield defect-related emissions in the wavelength range >300 nm.[18–22] Recent studies have shown that spontaneously formed AlGaN nanowire heterostructures with significantly improved optical and electrical properties can be realized via catalyst-free molecular beam epitaxy (MBE).[23–30,34–38] Nevertheless, the operation

[a]Electronic addresses: songrui.zhao@mail.mcgill.ca and zetian.mi@mcgill.ca. Telephone: +1 (514)398-7114.

wavelengths of LEDs and lasers using such spontaneously formed AlGaN nanowires have been limited to 250 nm, or longer.[28,35]

In the growth process of such spontaneously formed AlGaN nanowires, it involves the use of highly nitrogen rich conditions to promote the formation and nucleation of nanowire structures. However, due to the stronger binding energy of Al–N bond compared to Ga–N bond,[39] this nitrogen rich environment significantly reduces the Al adatom diffusion length, leading to highly nonuniform Al and Ga incorporation, which is evidenced by the commonly observed core-shell structures in AlGaN nanowires,[24,27,30,34,38] and the presence of significant compositional nonuniformity at the nano-[24,25,38,40] and atomic-scale.[34,35] This nonuniform Al and Ga incorporation significantly limits the wavelength tunability of AlGaN ternary nanowires in the UV-C band and prevents the realization of devices operating at a shorter wavelength.

In this paper, we show that MBE grown self-organized Al-rich AlGaN nanowires with relatively uniform compositional distribution can be achieved in a growth paradigm that is different from the conventional nitrogen rich conditions. This growth process involves the use of a GaN nanowire template to promote the formation of AlGaN nanowires, and subsequently a *low* nitrogen flow rate to enhance the surface migration of Al adatoms and thus the uniformity of Al/Ga compositional distribution, which is confirmed by scanning transmission electron microscopy (STEM) studies. We further show that, in this growth regime, a precise control on the optical bandgap of ternary AlGaN nanowires can be readily achieved by varying the substrate temperature, instead of changing Al and Ga beam equivalent pressures (BEPs) as in the conventional epitaxy process.[5–8,24,25,41] These findings provide a great promise to realize functional UV LEDs and lasers below 240 nm with AlGaN nanowires. In the end, as an example, we demonstrate ternary AlGaN nanowire LEDs with emission wavelengths in the range of 236 to 280 nm.

In this work, ternary AlGaN nanowire samples were grown by radio-frequency plasma-assisted MBE on Si substrate. Before the growth of the AlGaN segment, a GaN nanowire template was grown first, which provides an important dimension to control the growth process of the subsequent AlGaN nanowire segment. Figure 1(a) shows the schematic of the growth of AlGaN nanowire segment on such GaN nanowire template. For the growth of AlGaN segment, in order to enhance the Al migration, nitrogen flow rate was reduced to 0.4 standard cubic centimetre per minute (SCCM) compared to the previously reported value of 1 SCCM,[24,25,28,34,35] while both Al and Ga BEPs were kept at 2×10^{-8} Torr and substrate temperature (thermocouple reading) was in the range of 895–960 °C. Figure 1(c) shows the typical SEM image of such GaN/AlGaN nanowires. It is seen that highly uniform GaN/AlGaN nanowires, with an average height of 300 nm and diameter of 95 nm, can be formed. The nanowire density is about 2×10^{10} cm^{-3}. However, it is found that with such a low nitrogen flow rate, directly growing AlGaN nanowires on Si substrate without the GaN nanowire template only leads to highly coalesced nanowires and/or quasi-film-like structures, illustrated in Figs. 1(b) and 1(d). These results, therefore, suggest that the growth of AlGaN nanowire segment under low nitrogen flow rate in the present study is different from the conventional AlGaN nanowire growth in nitrogen rich conditions;[24,26,37,40] and it can be seen that with the use of GaN nanowire template, the subsequent growth of AlGaN nanowires does not necessarily require conventional nitrogen rich conditions.[24,26,37,40]

The detailed structural characterization of AlGaN nanowires was performed using a double aberration-corrected FEI Titan Cubed 80-300 STEM operated at 200 kV. Atomic-resolution, atomic-number sensitive (Z-contrast) STEM high-angle annular dark-field (HAADF) images were obtained using a detector angular range of 63.8–200 mrad. Elemental mapping by electron energy-loss spectroscopy (EELS) in STEM mode was done using the Ga $L_{2,3}$ and Al K-edges with the spectrum imaging technique. Weighted principal components analysis (PCA) was applied for noise reduction of the spectrum images using the MSA plugin implemented within DigitalMicrograph by HREM Research Inc. The nanowire samples were mechanically removed from Si substrate, and re-dispersed onto carbon-coated TEM support grids with anhydrous ethanol. Shown in Fig. 2(a) is a low-magnification STEM-HAADF image of a single GaN/AlGaN nanowire grown with a nitrogen flow rate of 0.4 SCCM and a substrate temperature of 950 °C. It is seen that AlGaN nanowire segment (darker region) is grown on GaN nanowire template (brighter region). The corresponding color-coded EELS elemental mapping shown in Fig. 2(b) highlights the Ga (blue) and Al (red)

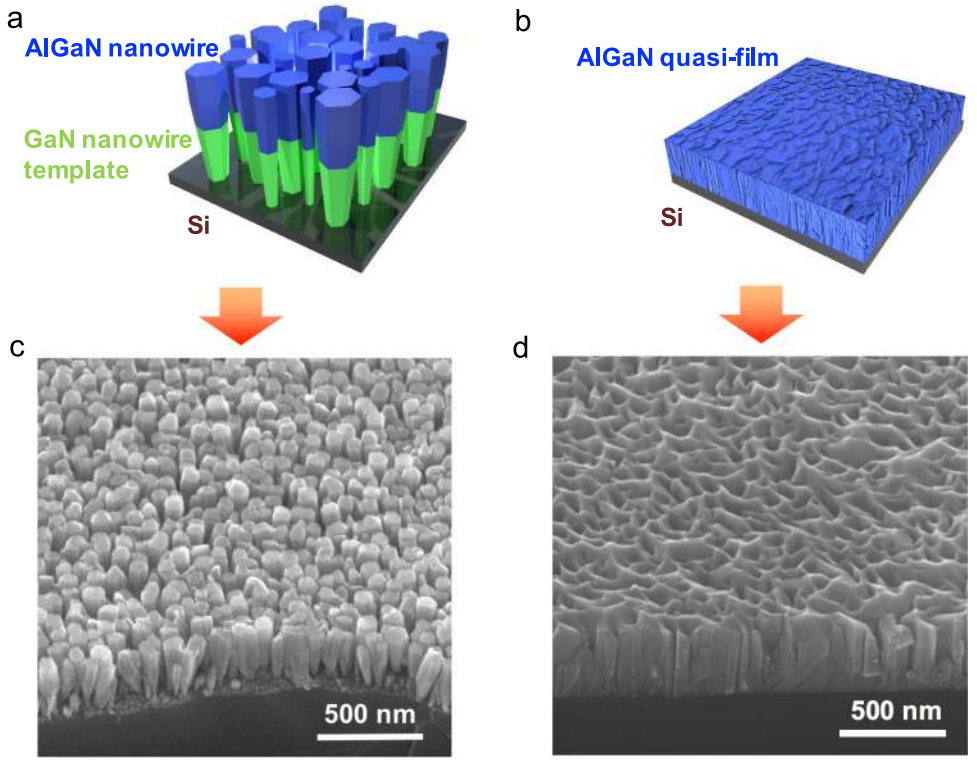

FIG. 1. MBE growth of AlGaN nanowires with a low nitrogen flow rate (0.4 SCCM). (a) Schematic of AlGaN nanowires grown on a GaN nanowire template on Si substrate. (b) Schematic of direct growth of AlGaN nanowires on Si substrate. (c) SEM image of GaN/AlGaN nanowires on Si. (d) SEM image of highly coalesced AlGaN nanowires grown directly on Si substrate. The SEM images were taken with a 45° tilting angle.

distributions within the nanowire. A sharp GaN/AlGaN interface is also measured, indicating the superior crystalline quality of the AlGaN nanowire segment. Figure 2(c) shows a high-resolution STEM-HAADF image near the top region of the AlGaN nanowire shown in Fig. 2(a). It is seen that the AlGaN segment exhibits relatively homogeneous image intensity, indicative of relatively uniform Al distribution. As a comparison, we have also studied the structural properties of GaN/AlGaN nanowires grown with similar conditions, except with a higher nitrogen flow rate (1.0 SCCM), i.e., in the conventional nitrogen rich condition for spontaneously formed nanowires by MBE. A low magnification STEM image of such a single nanowire is shown in Fig. 2(d), with the high-resolution image shown in the inset. Strong atomic-scale Al-/Ga-rich compositional modulations are evident, which are ascribed to the unique growth kinetics of AlGaN nanowires under nitrogen rich conditions.[34,35,38]

Therefore, these studies suggest the important role of nitrogen flow rate on the Al adatom incorporation. By reducing the nitrogen flow rate, Al adatom migration is enhanced, leading to significantly improved Al compositional uniformity, in contrast to AlGaN nanowires grown in the conventional nitrogen rich regime.[24,26,37,40] It has also been reported that with reducing nitrogen species, phase separation in AlGaN epilayers can be suppressed.[42] In addition, it is worthwhile mentioning that the detection limit for compositional variations from statistically random variations in this study is ~5 at.%. A small level of nano- or atomic-scale compositional modulation, coupled with the corresponding change in polarization field of AlGaN, may still exist and provide strong quantum-confinement of charge carriers.

Photoluminescence (PL) spectroscopy experiments were subsequently performed on a series of GaN/AlGaN nanowire samples grown with a nitrogen flow rate of 0.4 SCCM and substrate temperatures varying from 895 to 960 °C. Al and Ga BEPs were kept at 2×10^{-8} Torr. In the PL measurements, the nanowires were optically excited using a 193 nm ArF excimer laser. The laser spot size was about 1 mm^2. The emitted light from the nanowires was collected by

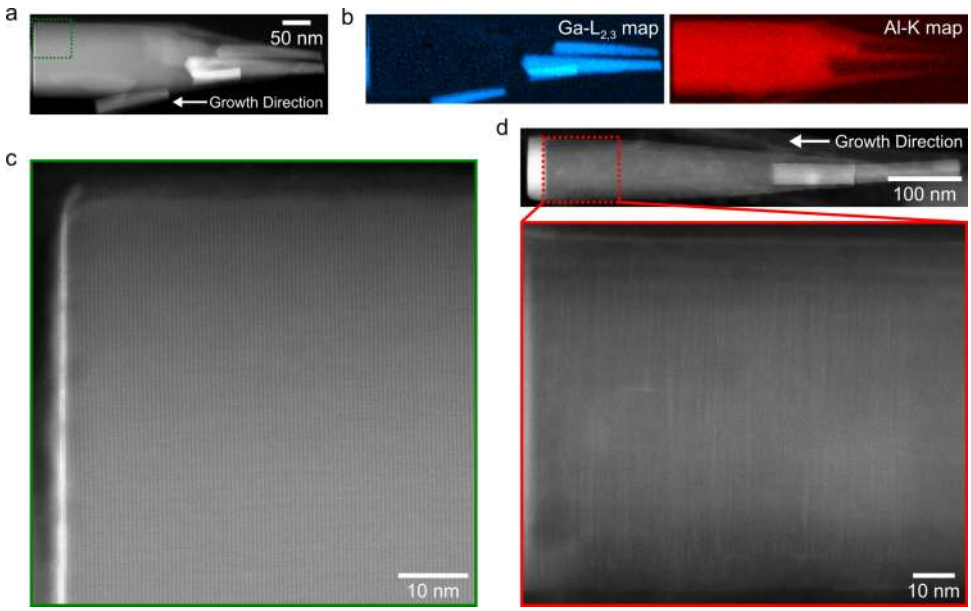

FIG. 2. Structural properties of AlGaN nanowires. (a) A low-magnification STEM image of a single GaN/AlGaN nanowire grown with a low nitrogen flow rate (0.4 SCCM), and (b) the corresponding color-coded EELS maps showing the elemental distribution of Ga and Al. (c) A high-resolution image taken from the AlGaN segment in (a), manifesting the relatively uniform Al distribution. The thin bright band is the p-GaN contact layer. (d) A low-magnification STEM image of a single GaN/AlGaN nanowire grown with a high nitrogen flow rate (1.0 SCCM), with the inset showing a high-resolution image taken from the AlGaN segment, highlighting the strong atomic-scale compositional modulation.

a fused silica lens and spectrally resolved by a high-resolution spectrometer, and then detected by a liquid nitrogen cooled CCD camera. Figure 3(a) shows the PL spectra measured at room temperature. It is seen that the emission wavelength exhibits a progressive blueshift with increasing substrate temperature. At a growth temperature of 960 °C, AlGaN nanowires with emission wavelength at 232 nm are achieved, with a spectral linewidth (full-width-half-maximum—FWHM) of 16 nm. Al composition can be approximated by the room-temperature PL peak energy E_{PL} via $E_{PL}(x) \approx E_g(x) = (1-x)E_g(GaN) + xE_g(AlN) - bx(1-x)$, where x is the Al composition, E_g is the bandgap energy, and b is bowing parameter that is generally in the range of 0.6-1.3 eV.[43–46] In the present work, b is taken to be 1 eV, $E_g(GaN)$ and $E_g(AlN)$ are 3.4 and 6.2 eV, respectively. Figure 3(b) shows the PL peak wavelength *vs*. Al content x, which is consistent with previous reports.[24,47] In addition, it is noted that due to the presence of Al-rich AlGaN shell, the average Al content should be higher than what is estimated here.

We have further investigated optical properties of an AlGaN nanowire sample grown under similar conditions as the sample emitting at 232 nm, except that the nitrogen flow rate was increased

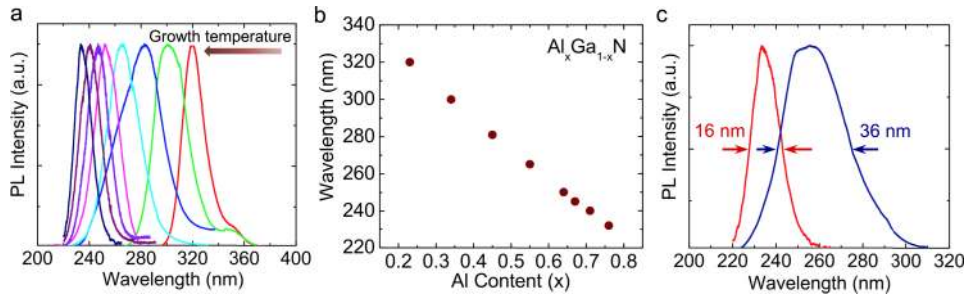

FIG. 3. PL properties of AlGaN nanowires. (a) PL spectra of samples grown under different substrate temperatures (895 °C to 960 °C) with a nitrogen flow rate of 0.4 SCCM. The arrow indicates the growth temperature increase direction. (b) PL peak wavelength *vs*. Al content. (c) PL spectrum (blue curve) of a sample grown with the similar condition as the sample emitting at 232 nm in (a) (also shown in (c), red curve), but with a nitrogen flow rate of 1.3 SCCM.

to 1.3 SCCM. As illustrated in Fig. 3(c), it is seen that the PL peak is red-shifted to around 253 nm, with a significantly broader linewidth (FWHM) of 36 nm. This broad linewidth is similar to previous reports,[24,34] and is attributed to inhomogeneous broadening associated with highly nonuniform Al (and Ga) distribution when grown under nitrogen rich conditions (also see Fig. 2(d)).

The compositional nonuniformity makes it difficult to achieve optical emission in the wavelength range of 240 nm in previous studies. In this work, by growing AlGaN nanowires with low nitrogen flow rate, we have discovered that the optical bandgap (and thus the emission wavelength) of AlGaN nanowires can be precisely tuned by simply varying the substrate temperature, instead of changing the Al/Ga BEP ratio in the conventional process.[24,25,41] A consistent blueshift of the PL emission wavelength with increasing growth temperature, shown in Fig. 3(a), is directly related to the enhanced Ga adatom desorption and therefore reduced incorporation in the nanowire.

This precise control on the optical bandgap of ternary AlGaN nanowires with the aforediscussed nonconventional approach provides a great promise to realize AlGaN nanowire deep UV optoelectronic devices, in particular LEDs and lasers below 240 nm, which have remained challenging today. In the end, as an example, we show Al-rich AlGaN nanowire LEDs in the UV-C band, and more importantly, AlGaN nanowire LEDs emitting below 240 nm are also demonstrated for the first time. The device schematic is shown in Fig. 4(a). The device active region consists of 40 nm undoped AlGaN, surrounded by *p*- and *n*-doped AlGaN cladding layers. Si (*n*-type dopants) and Mg (*p*-type dopants) doping concentrations were around 2×10^{19} cm^{-3} and 2×10^{20} cm^{-3}, respectively.[26,31] A very thin (3 nm) GaN layer was deposited as the *p*-contact layer. For device fabrication, 10 nm Ti/30 nm Au metal layers were deposited onto the backside of *n*-Si substrate with an e-beam evaporator. The sample was then patterned into devices by optical lithography. No filling materials were utilized in this work, to avoid any light absorption in the UV-C spectral range. The top *p*-metal contact (10 nm Ni/10 nm Au), with a size of 500 μm × 500 μm, was deposited also by

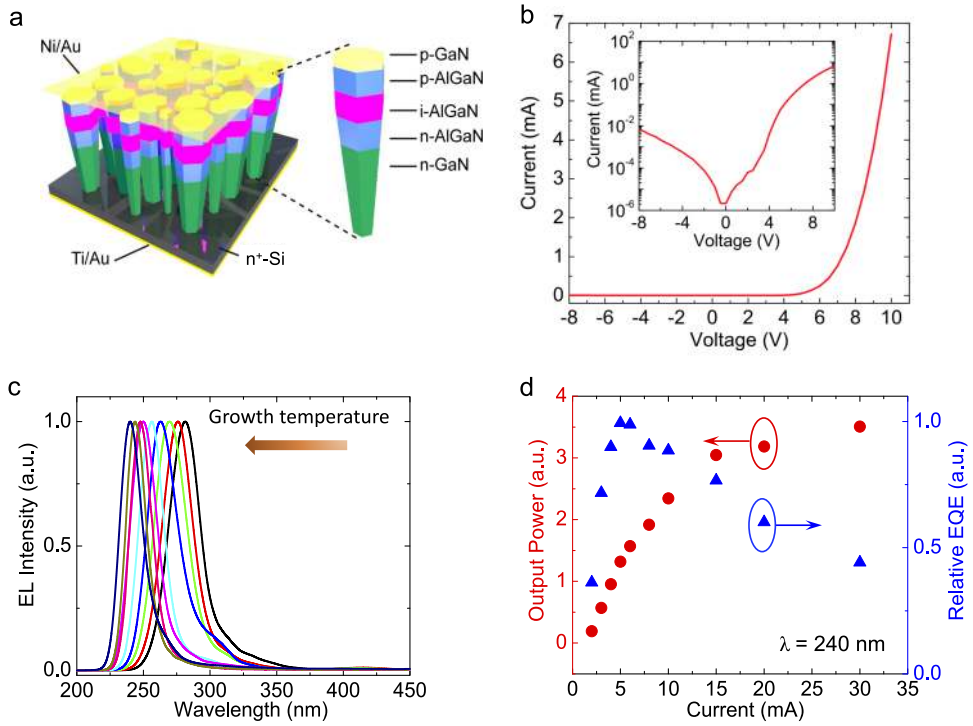

FIG. 4. Characteristics of AlGaN nanowire LEDs. The *p*-metal size is 500 μm × 500 μm. (a) Schematic of AlGaN nanowire LEDs. (b) I-V characteristics of AlGaN nanowire LEDs emitting around 240 nm, with the inset showing the plot in a semi-log scale. (c) EL spectra measured from AlGaN nanowire LEDs with different emission wavelengths, under an injection current of 20 mA. The arrow indicates the increase of growth temperature for AlGaN active layers. (d) The light output power and relative EQE *vs*. injection current of a device emitting around 240 nm.

e-beam evaporation, with a tilting angle. The devices were measured with a Keithley 2400 source meter unit under continuous-wave (CW) biasing.

The current-voltage (I-V) characteristics of an AlGaN nanowire LED device with emission wavelength around 240 nm are shown in Fig. 4(b). The device has a turn on voltage slightly over 5 V. The inset of Fig. 4(b) shows the I-V characteristics in a semi-log scale. The excellent current conduction in such an Al-rich AlGaN nanowire LED is directly related to the significantly enhanced Mg-dopant incorporation in the nanowire structure and the resultant Mg impurity band conduction.[48,49] The room-temperature electroluminescence (EL) spectra measured from different devices are shown in Fig. 4(c). The emitted light was collected from the device top surface by a deep UV optical fibre and detected by a CCD camera. It is seen that by changing the growth temperature of the device active region, the emission wavelength of AlGaN nanowire LEDs can be precisely tuned from 236 to 280 nm. Moreover, for all the devices measured, there is no defect emission in the UV spectral range, and only negligible emission around 480 nm is measured. The light output power *vs.* injection current of a device emitting around 240 nm is shown in Fig. 4(d) (red circles). It is seen that the light intensity increases nearly linearly up to 15 mA. A maximum light output power around 100 nW is measured. The relative external quantum efficiency (EQE, defined by the light intensity over current in the present study) is also shown in Fig. 4(d) (blue triangles). A droop behavior is clearly seen, which is largely attributed to electron overflow, due to the highly asymmetric electron and hole transport in Al-rich AlGaN and the absence of electron blocking layer.

In summary, we have established an epitaxy process of self-organized GaN/AlGaN nanowire heterostructures to achieve tunable emission in the deep UV spectral range. By employing a GaN nanowire template and growing AlGaN nanowires with a low nitrogen flow rate, the Al/Ga compositional uniformity is significantly improved, and the optical bandgap (and thus the emission wavelength) of ternary AlGaN nanowires can be readily tuned by varying the substrate temperature, instead of by changing the Al/Ga BEP ratio. These findings not only represent a critical step towards achieving UV LEDs and lasers below 240 nm with AlGaN nanowire technologies, but are also important for the growth and synthesis of other semiconductor nanostructures. As an example, we have demonstrated AlGaN nanowire LEDs with emission wavelengths in the UV-C band, including the spectral range below 240 nm, which was not possible previously with AlGaN nanowires. Future work includes the development of high power AlGaN nanowire UV LEDs and lasers below 240 nm, which are extremely important for a wide range of applications in biochemical and medical sciences.

This work was supported by the Natural Sciences and Engineering Research Council of Canada and US Army Research Office under Grant No. W911NF-15-1-0168. Part of the work was performed in the McGill Nanotools-Microfab facility and Facility for Electron Microscopy Research. STEM and EELS investigations were performed at the Canadian Centre for Electron Microscopy, a national facility supported by NSERC, the Canada Foundation for Innovation under the MSI program, and McMaster University. The authors would like to thank Mr. X. Liu for the help on schematics.

[1] Y. Taniyasu, M. Kasu, and T. Makimoto, Nature **441**, 325 (2006).
[2] M. Kneissl, Z. Yang, M. Teepe, C. Knollenberg, O. Schmidt, P. Kiesel, N. M. Johnson, S. Schujman, and L. J. Schowalter, J. Appl. Phys. **101**, 123103 (2007).
[3] H. Yoshida, Y. Yamashita, M. Kuwabara, and H. Kan, Appl. Phys. Lett. **93**, 241106 (2008).
[4] H. Yoshida, Y. Yamashita, M. Kuwabara, and H. Kan, Nat. Photonics **2**, 551 (2008).
[5] H. Hirayama, N. Maeda, S. Fujikawa, S. Toyoda, and N. Kamata, Jpn. J. Appl. Phys., Part 1 **53**, 100209 (2014).
[6] M. Kneissl, T. Kolbe, C. Chua, V. Kueller, N. Lobo, J. Stellmach, A. Knauer, H. Rodriguez, S. Einfeldt, Z. Yang, N. M. Johnson, and M. Weyers, Semicond. Sci. Technol. **26**, 014036 (2011).
[7] A. Khan, K. Balakrishnan, and T. Katona, Nat. Photonics **2**, 77 (2008).
[8] Y. Muramoto, M. Kimura, and S. Nouda, Semicond. Sci. Technol. **29**, 084004 (2014).
[9] X.-H. Li, T. Detchprohm, T.-T. Kao, M. M. Satter, S.-C. Shen, P. Douglas Yoder, R. D. Dupuis, S. Wang, Y. O. Wei, H. Xie, A. M. Fischer, F. A. Ponce, T. Wernicke, C. Reich, M. Martens, and M. Kneissl, Appl. Phys. Lett. **105**, 141106 (2014).
[10] H. Sun, J. Woodward, J. Yin, A. Moldawer, E. F. Pecora, A. Y. Nikiforov, L. Dal Negro, R. Paiella, K. Ludwig, D. J. Smith, and T. D. Moustakas, J. Vac. Sci. Technol., B: Microelectron. Nanometer Struct. **31**, 03C117 (2013).
[11] Y. Liao, C.-k. Kao, C. Thomidis, A. Moldawer, J. Woodward, D. Bhattarai, and T. D. Moustakas, Phys. Status Solidi C **9**, 798 (2012).
[12] J. Xie, S. Mita, Z. Bryan, W. Guo, L. Hussey, B. Moody, R. Schlesser, R. Kirste, M. Gerhold, R. N. Collazo, and Z. Sitar, Appl. Phys. Lett. **102**, 171102 (2013).

[13] H. Taketomi, Y. Aoki, Y. Takagi, A. Sugiyama, M. Kuwabara, and H. Yoshida, Jpn. J. Appl. Phys., Part 1 **55**, 05FJ05 (2016).
[14] H. Hirayama, S. Fujikawa, N. Noguchi, J. Norimatsu, T. Takano, K. Tsubaki, and N. Kamata, Phys. Status Solidi A **206**, 1176 (2009).
[15] C. Reich, M. Guttmann, M. Feneberg, T. Wernicke, F. Mehnke, C. Kuhn, J. Rass, M. Lapeyrade, S. Einfeldt, A. Knauer, V. Kueller, M. Weyers, R. Goldhahn, and M. Kneissl, Appl. Phys. Lett. **107**, 142101 (2015).
[16] J.-I. Chyi, H. Fujioka, H. Morkoç, M. Lapeyrade, F. Eberspach, J. Glaab, N. Lobo-Ploch, C. Reich, C. Kuhn, M. Guttmann, T. Wernicke, F. Mehnke, S. Einfeldt, A. Knauer, M. Weyers, and M. Kneissl, Proc. SPIE **9363**, 93631P (2015).
[17] S. Okawara, Y. Aoki, Y. Yamashita, and H. Yoshida, in 6th International Symposium on Growth of III-Nitrides (ISGN-6), 2015.
[18] L. Hong, Z. Liu, X. T. Zhang, and S. K. Hark, Appl. Phys. Lett. **89**, 193105 (2006).
[19] C. He, Q. Wu, X. Wang, Y. Zhang, L. Yang, N. Liu, Y. Zhao, Y. Lu, and Z. Hu, ACS Nano **5**, 1291 (2011).
[20] F. Chen, X. Ji, Z. Lu, Y. Shen, and Q. Zhang, Mater. Sci. Eng. B **183**, 24 (2014).
[21] F. Ye, X.-M. Cai, X. Zhong, H. Wang, X.-Q. Tian, D.-P. Zhang, P. Fan, J.-T. Luo, Z.-H. Zheng, and G.-X. Liang, J. Alloys Compd. **620**, 87 (2015).
[22] A. K. Sivadasan, A. Patsha, S. Polaki, S. Amirthapandian, S. Dhara, A. Bhattacharya, B. K. Panigrahi, and A. K. Tyagi, Cryst. Growth Des. **15**, 1311 (2015).
[23] K. A. Bertness, A. Roshko, N. A. Sanford, J. M. Barker, and A. V. Davydov, J. Cryst. Growth **287**, 522 (2006).
[24] A. Pierret, C. Bougerol, S. Murcia-Mascaros, A. Cros, H. Renevier, B. Gayral, and B. Daudin, Nanotechnology **24**, 115704 (2013).
[25] C. Himwas, M. den Hertog, L. S. Dang, E. Monroy, and R. Songmuang, Appl. Phys. Lett. **105**, 241908 (2014).
[26] S. Zhao, A. T. Connie, M. H. Dastjerdi, X. H. Kong, Q. Wang, M. Djavid, S. Sadaf, X. D. Liu, I. Shih, H. Guo, and Z. Mi, Sci. Rep. **5**, 8332 (2015).
[27] Q. Wang, A. T. Connie, H. P. T. Nguyen, M. G. Kibria, S. Zhao, S. Sharif, I. Shih, and Z. Mi, Nanotechnology **24**, 345201 (2013).
[28] T. F. Kent, S. D. Carnevale, A. T. Sarwar, P. J. Phillips, R. F. Klie, and R. C. Myers, Nanotechnology **25**, 455201 (2014).
[29] S. D. Carnevale, T. F. Kent, P. J. Phillips, M. J. Mills, S. Rajan, and R. C. Myers, Nano Lett. **12**, 915 (2012).
[30] K. H. Li, X. Liu, Q. Wang, S. Zhao, and Z. Mi, Nat. Nanotechnol. **10**, 140 (2015).
[31] S. Zhao, B. H. Le, D. P. Liu, X. D. Liu, M. G. Kibria, T. Szkopek, H. Guo, and Z. Mi, Nano Lett. **13**, 5509 (2013).
[32] S. Zhao, S. Fathololoumi, K. H. Bevan, D. P. Liu, M. G. Kibria, Q. Li, G. T. Wang, H. Guo, and Z. Mi, Nano Lett. **12**, 2877 (2012).
[33] Z. Fang, E. Robin, E. Rozas-Jimenez, A. Cros, F. Donatini, N. Mollard, J. Pernot, and B. Daudin, Nano Lett. **15**, 6794 (2015).
[34] S. Zhao, S. Y. Woo, M. Bugnet, X. Liu, J. Kang, G. A. Botton, and Z. Mi, Nano Lett. **15**, 7801 (2015).
[35] S. Zhao, X. Liu, S. Y. Woo, J. Kang, G. A. Botton, and Z. Mi, Appl. Phys. Lett. **107**, 043101 (2015).
[36] S. Zhao, M. Djavid, and Z. Mi, Nano Lett. **15**, 7006 (2015).
[37] S. D. Carnevale, T. F. Kent, P. J. Phillips, A. T. Sarwar, C. Selcu, R. F. Klie, and R. C. Myers, Nano Lett. **13**, 3029 (2013).
[38] A. Pierret, C. Bougerol, M. den Hertog, B. Gayral, M. Kociak, H. Renevier, and B. Daudin, Phys. Status Solidi RRL **7**, 868 (2013).
[39] E. Iliopoulos and T. D. Moustakas, Appl. Phys. Lett. **81**, 295 (2002).
[40] C. Himwas, M. den Hertog, F. Donatini, L. S. Dang, L. Rapenne, E. Sarigiannidou, R. Songmuang, and E. Monroy, Phys. Status Solidi C **10**, 285 (2013).
[41] J. Ristic, M. A. Sanchez-Garcia, E. Calleja, J. Sanchez-Paramo, J. M. Calleja, U. Jahn, and K. H. Ploog, Phys. Status Solidi A **192**, 60 (2002).
[42] M. Iwaya, S. Terao, T. Sano, T. Ukai, R. Nakamura, S. Kamiyama, H. Amano, and I. Akasaki, J. Cryst. Growth **237–239**, 951 (2002).
[43] F. Yun, M. A. Reshchikov, L. He, T. King, H. Morkoç, S. W. Novak, and L. Wei, J. Appl. Phys. **92**, 4837 (2002).
[44] H. Jiang, G. Y. Zhao, H. Ishikawa, T. Egawa, T. Jimbo, and M. Umeno, J. Appl. Phys. **89**, 1046 (2001).
[45] S. R. Lee, A. F. Wright, M. H. Crawford, G. A. Petersen, J. Han, and R. M. Biefeld, Appl. Phys. Lett. **74**, 3344 (1999).
[46] H. Angerer, D. Brunner, F. Freudenberg, O. Ambacher, M. Stutzmann, R. Höpler, T. Metzger, E. Born, G. Dollinger, A. Bergmaier, S. Karsch, and H. J. Körner, Appl. Phys. Lett. **71**, 1504 (1997).
[47] Q. Wang, H. P. T. Nguyen, K. Cui, and Z. Mi, Appl. Phys. Lett. **101**, 043115 (2012).
[48] A. T. Connie, S. Zhao, S. M. Sadaf, I. Shih, Z. Mi, X. Du, J. Lin, and H. Jiang, Appl. Phys. Lett. **106**, 213105 (2015).
[49] R. J. Molnar, T. Lei, and T. D. Moustakas, Appl. Phys. Lett. **62**, 72 (1993).